Proc. Nat. Acad. Sci. USA
Vol. 72, No. 8, pp. 2886–2890, August 1975
Biochemistry

Interaction of ubisemiquinone with a paramagnetic component in heart tissue

(flavin semiquinone/high potential iron-sulfur protein/dipole–dipole interaction/spectrum simulation)

FRANK J. RUZICKA*, HELMUT BEINERT*, KENNETH L. SCHEPLER†, W. RICHARD DUNHAM†, AND RICHARD H. SANDS†

* Institute for Enzyme Research, University of Wisconsin, Madison, Wisc. 53706; and † Biophysics Research Division, Institute of Science and Technology, University of Michigan, Ann Arbor, Mich. 48105

Communicated by David E. Green, April 28, 1975

ABSTRACT The origin of most of the electron paramagnetic resonances obtained at low temperature and low microwave power from heart tissue and subcellular fractions derived therefrom is now understood. A signal that emerges on partial reduction with characteristic lines at 3227 G (0.3227 tesla) and 3309 G (0.3309 tesla) (at 9.2 GHz) and disappears again on full reduction has remained unidentified. According to its behavior on oxidation-reduction, the substance giving rise to this signal has the properties of a two-electron acceptor. The signal is strongly dependent on temperature and can only be well resolved at <20°K. It is readily elicited in submitochondrial particles by partial reduction, but has not been observed in submitochondrial particles from which ubiquinone has been removed by pentane extraction. When ubiquinone is reincorporated into extracted submitochondrial particles, the signal is again easily produced by partial reduction. Electron paramagnetic resonance spectra of partially reduced submitochondrial particles recorded at 34 GHz show lines centered about $g \sim 2$ with the same separation (~82 G; ~0.0082 tesla) as do 9.2 GHz spectra, whereas no lines are detected with a separation of approximately 82 × 34/9.2 G (0.0082 × 34/9.2 tesla). We suggest, on the basis of these observations, that the unidentified signal arises from an interaction of ubisemiquinone and a second paramagnetic species. Three obvious choices exist concerning this second species: ubisemiquinone, flavin semiquinone, or an iron-sulfur center. It is not possible without much additional information to decide between these possibilities. Since we have never observed the signal in the absence of the membrane-bound, high-potential type iron-sulfur protein, we have considered involvement of this species in the interaction. However, according to computer simulations of the observed electron paramagnetic resonance spectra, which yield best fits for semiquinone-semiquinone interaction, the possibility that ubi- or flavin semiquinone is the interaction partner appears more likely at this time. The interaction appears to be of the magnetic dipole–dipole type, but it is not certain whether there is also a contribution from spin exchange coupling. If it is assumed that the signal is due to magnetic dipole–dipole interaction, the distance of the partners is ≤7.7 Å.

In recent efforts in our laboratory (1, 2) to identify the electron paramagnetic resonance (EPR) detectable components of heart mitochondria, the EPR signals of two unidentified electron acceptors and their response to oxidation-reduction were described. These signals were also seen in whole heart tissue, excluding any artifactual origin. These signals show derivative peaks at 3253 G (max) (0.3253 tesla) and 3281 G (min) (0.3281 tesla) and at 3227 G (max) (0.3227 tesla) and 3309 G (min) (0.3309 tesla), at 9.213 GHz, respectively (see Fig. 1). Both signals are very sensitive to temperature. They are only detectable at temperatures below 25°K. The species with peaks at 3253 and 3281 G (0.3253 and 0.3281 tesla) is typical for the oxidized state and has been seen in a number of preparations and organisms (3–5). We have recently identified this species as an iron-sulfur (Fe-S) protein of the general type of "high-potential" Fe-S proteins (Hipip) (6). The unidentified signal with peaks at 3227 and 3309 G (0.3227 and 0.3309 tesla) characteristically only appeared at states of partial reduction and disappeared again on full reduction (see ref. 1, Fig. 1 and ref. 2, Fig. 5), i.e., it behaved as expected of a two-electron acceptor, such as a semiquinone. However, the same behavior might be shown if the signal were due to the interaction of a reduced and an oxidized paramagnetic species. The temperature sensitivity of the signal is typical for transition metals rather than for semiquinones, but metal components that are two-electron acceptors are not known to occur at the required concentration in heart. It seemed possible, therefore, that the signal might arise from the interaction of semiquinone species or a semiquinone and metal. In submitochondrial particles (ETP) semiquinones may be formed from flavin or ubiquinone (Q). Since the signal was not observed in partly reduced flavoproteins of mitochondrial origin that are low in Q, such as succinate-Q reductase (Complex II), or in nonmitochondrial (metal −) flavoproteins, our attention was focussed on Q.

Bäckström *et al.* (7) have shown that the intensity of the free radical signal in partly reduced submitochondrial particles is decreased after removal and restored after reincorporation of Q into the particles. By analogous extraction and reconstitution procedures we could show that the appearance of the unidentified signal in ETP indeed depends on the presence of Q. However, when ETP are further fractionated, e.g., into Complexes I to III, not all fractions that contain ample Q, such as Complex I, show the characteristic lines on partial reduction. The lines have thus far only been seen in materials that also contain the membrane-bound Hipip species (6) and they disappear on reduction with the disappearance of the Hipip signal. We suggest, therefore, that the unidentified signal is either due to an interaction of ubisemiquinone (SQ) with mitochondrial Hipip or to interaction of two SQ molecules, or of SQ and flavin semiquinone in which mitochondrial Hipip may play an as yet undefined role.

Abbreviations: EPR, electron paramagnetic resonance; Fe-S, iron-sulfur; Q, ubiquinone; SQ, ubisemiquinone; ETP, submitochondrial particles; Hipip, high potential Fe-S protein.

MATERIALS AND METHODS

Beef heart mitochondria were prepared according to Crane *et al.* (8). Preparation of ETP was as described by Ruzicka

Table 1. Ubiquinone-10 content and succinoxidase and DPNH oxidase activities of intact, extracted, and reconstituted ETP

	DPNH oxidase	Succin-oxidase	Q-10
	μg-atom oxygen/ (min × mg protein)		nmol/ mg protein
Fresh	2.01	0,94	4.2
Lyophilized	1.27	0.83	3.9
Extracted	0.05	0.10	<0.05
Reconstituted	0.92	0.84	6.1

and Beinert (6) with the following modification. After sonication, the suspensions were centrifuged at 48,000 × *g* for 15 min. The supernatant was then centrifuged at 78,000 × *g* for 2 hr. The pellets, which contained the electron transport particles (ETP), were resuspended in 0.15 M KCl prior to lyophilization and pentane extraction. Pentane extraction and Q-10 reincorporation were as described by Norling *et al.* (9). Extracted particles (800 mg dry weight) were added to 60 ml of dry *n*-pentane containing 7.5 mg of Q-10. Q analysis was carried out according to Kröger and Klingenberg (10). DPNH oxidase and succinoxidase activities were determined polarographically at 30° in the presence of 40 mM Tris·HCl (pH 7.4), 13 μM cytochrome *c*, 10 μM EDTA, 20 mM succinate or 0.8 mM DPNH. Anaerobic reductive titrations and EPR spectroscopy were carried out as described (1, 2).

RESULTS

Appearance of unidentified signal and ubiquinone content

Table 1 presents characteristics of the preparations used. Fig. 1 shows EPR spectra at 9.2 GHz of lyophilized intact (A), pentane-extracted (B), and extracted and reconstituted (C) particles, all after partial reduction with dithionite. According to our previous work (2), the signal of the unknown species is observed over a relatively broad range of oxidation states. Guided by the information from the previous work, we never failed to elicit the typical EPR spectrum of the unknown species in intact or reconstituted particles by addition of DPNH or dithionite over a considerable range (4.2–9.7 neq/mg of protein). On the other hand, over an even broader range (1.8–36 neq/mg) we never succeeded in producing the spectrum characterized by peaks at 3227 G (0.3227 tesla) and 3309 G (0.3309 tesla) in extracted preparations. Although after extraction of Q the number of reducing equivalents required for corresponding reduction is less than in intact or reconstituted particles, we can compare oxidation states by observation of signals at $g = 1.92$ (reduced Fe-S center 2 of DPNH dehydrogenase), 1.89 (reduced Fe-S protein of b-c_1 complex), and of the copper and Hipip signals at $g \sim 2$.

Evidence that unidentified signal originates from interaction

If the typical lines observed at 9.2 GHz at 3227 and 3309 G (0.3227 and 0.3309 tesla) were due to the interaction of two paramagnetic species, their separation [82 G (0.0082 tesla) at 9.2 GHz] should not change with changing microwave frequency; if these lines, however, represented features due to anisotropy of an independent paramagnet, they should be separated 33.9/9.2 = 3.69-fold at 33.9 GHz as compared to 9.2 GHz. Fig. 2 C-E shows EPR spectra recorded at 33.9 GHz of two ETP samples that are at a somewhat different oxidation state and hence show the signals of Hipip and the unknown lines at a different state of development. The 9.2 GHz spectra of the same samples are shown in Fig. 2A and B. As can be seen from the intensity of the line at 3427 G (0.3427 tesla), which represents reduced Fe-S center 2 of DPNH dehydrogenase, sample B (D) is more reduced. Both sets of spectra, those recorded at low and high frequency, are presented with the same expansion of the abscissa (gauss), so that the line of center 2 at 3427 G (0.3427 tesla) would be off to the right in the 33.9 GHz spectra C and D. For orientation, the sample of curves A and C is shown in Fig. 2E in a recording at 33.9 GHz, but at a 2.5-fold condensed scale on the abscissa so that reduced center 2 [3427 G (0.3427 tesla) at 9.2 GHz] is again in the field to the right.

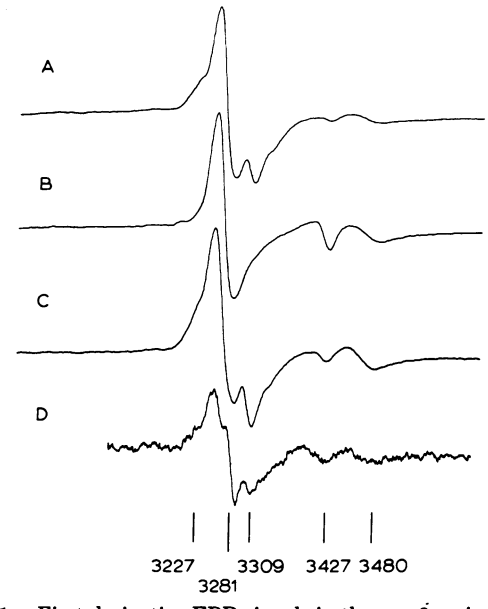

FIG. 1. First derivative EPR signals in the $g = 2$ region of typical samples of lyophilized, extracted, and reconstituted ETP, partly reduced with dithionite. For corresponding analytical data see Table 1. (A) Lyophilized ETP (30 mg of protein per ml of medium); (B) lyophilized, pentane-extracted ETP; (C and D) lyophilized, pentane-extracted ETP after reconstitution with Q-10. The conditions of EPR spectroscopy were: microwave power, 2.7 mW, but 27 μW for D; frequency 9.218 GHz; modulation frequency 100 kHz; amplitude, 8 G (8 × 10^{-4} tesla); temperature 13.3 ± 0.2 K; scanning rate 400 G (0.04 tesla) per min; and time constant 0.5 sec. The field positions of prominent peaks in the spectra are indicated in G.

If we were dealing with anisotropic features of a single paramagnetic species and if we assume the same field position for the center of the lines at both frequencies, they should appear in the 33.9 GHz spectra where indicated by broken arrows (Fig. 2C-E). No lines are seen in these regions. There are, however, two weak lines, particularly visible in Fig. 2C, which are symmetrically disposed around the center of the Hipip and semiquinone signals with a separation of ~82 G (~0.0082 tesla). We assume that these lines correspond to those observed at 9.2 GHz with an 82 G (0.0082 tesla) separation. We have seen these lines consistently in computer-averaged spectra of a number of samples, excluding any fortuitous appearance.

Type of interaction

Two types of interaction might be involved, namely, interaction between magnetic dipoles or exchange interaction,

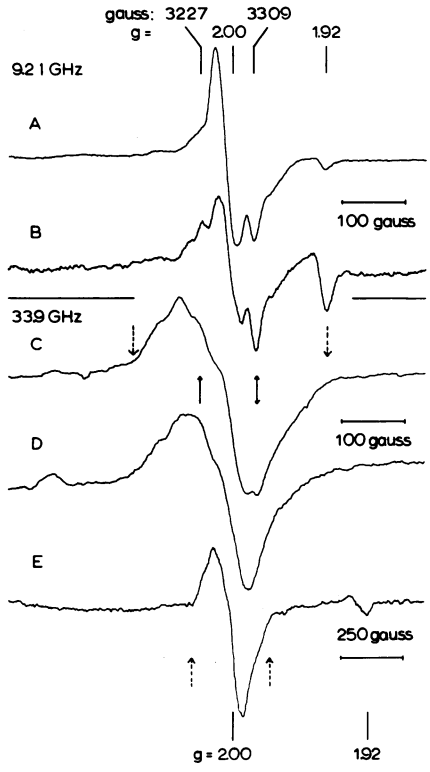

FIG. 2. First derivative EPR spectra of ETP at two states of partial reduction and at different microwave frequencies. ETP (50 mg/ml of medium) was partially reduced with dithionite. The samples used for curves A, C, and E and for B and D are identical. Sample B (D) is more reduced. The conditions of EPR spectroscopy were: for A and B as for Fig. 1A except that the microwave frequency was 9.233 GHz. For C and D the microwave power was 0.61 mW, the frequency 33.99 GHz, the modulation frequency 100 kHz; amplitude 6.3 G (6.3×10^{-4} tesla); temperature 13.3 ± 0.2 K; time constant 0.5 sec; and scanning rate 400 G (0.04 tesla) per min. The total field scanned was the same for A-D but for E it was 2500 G (0.25 tesla) instead of 1000 G (0.1 tesla). Prominent features are marked as in Fig. 1. The *g*-values on top of the figure refer to spectra A and B, those at the bottom to spectrum E. The *solid arrows* point to the resonance lines of the unidentified signal, the *broken arrows* point to those positions where the lines observed at 9.24 GHz should be found at 33.9 GHz if they were due to anisotropic features of an independent paramagnetic species.

which is an electrostatic effect. The former is anisotropic by its very nature, the latter may or may not have an anisotropic component. From the information that can be obtained at present from the rather complex materials under study, it is not possible to say whether in addition to dipolar coupling there is a contribution from spin exchange interaction (see ref. 11). In either one of these cases, however, two sets of lines should be observed with a common center, an approximately equal separation between lines, and with the outer lines being weaker than those close to the center (see next section). Since the spectra we observe (Figs. 1–3) are in fact superpositions of spectra stemming from the noninteracting parent species and the interacting pairs, only reconstruction of the spectra by computation can decide which lines of the two sets of lines that are expected, are represented by the prominent ones at 3227 and 3309 G (0.3227 and 0.3309 tesla) at 9.2 GHz, which we observe. As apparent from Figs. 1 and 2, with ETP there are additional signals superimposed not related to those under consideration. As a basis for computations we have, therefore, chosen the signal observed when reduced Complex II is partly reoxidized by a Q analog

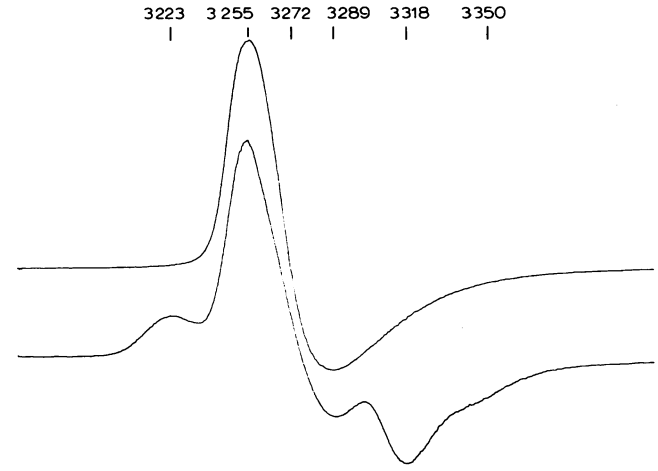

FIG. 3. EPR spectra of succinate-ubiquinone reductase (Complex II) in the oxidized state (upper curve) and 100 msec after reaction of Complex II, previously reduced with dithionite, with a Q analog (lower curve). Complex II, in 0.05 M *N*-2-hydroxyethylpiperazine-*N'*-2-ethanesulfonic acid (Hepes) buffer of pH 7.8, containing 22 μmol of bound flavin per ml, was reduced with 4 mol of dithionite per mol of flavin and then rapidly mixed with an equal volume of 0.24 mM 2,3-dimethoxy-5-methyl-6-pentyl-1,4-benzoquinone. The conditions of microwave spectroscopy were: microwave power, 9 mW; modulation amplitude 8 G (8×10^{-4} tesla); scanning rate, 50 G (5×10^{-3} tesla) per min; time constant 0.5 sec; and temperature, 10 K. The frequency was 9.214 GHz.

(Fig. 3; with Complex II the characteristic signal has only been observed under these conditions). With Complex II, interference by copper and iron-sulfur protein signals is minimal. All the lines observed in the lower spectrum of Fig. 3 must be considered, therefore.

Computer simulation of spectrum

It is possible to see from the experimental spectra shown in Figs. 1–3 that the previously unidentified spectra arise from dipole-dipole interactions between two $S = \frac{1}{2}$ species. This becomes obvious when the superimposed EPR spectrum for noninteracting Hipip (Fig. 4A) is subtracted from the experimental spectrum, leaving a spectrum similar to that shown in Fig. 4B. Such a spectrum is reminiscent of the spectra observed in wideline nuclear magnetic resonance for two dipolar coupled protons (see ref. 12), with only a slight additional anisotropy.

The situation here differs from the case of two coupled protons in two important respects: (*i*) the *g*-tensors of the interacting spin systems can be anisotropic and (*ii*) the interacting spin systems have dimensions of the same order as the distance between them. Because both of these features only complicate the mathematics and add little to our present understanding, we will begin by describing the spectra to be expected from two point electrons with identical isotropic *g*-tensors, interacting by means of the magnetic dipole-dipole interaction. The added complications caused by the electrons having anisotropic *g*-tensors and distributed moments will be discussed last. The former case is exactly analogous to the case of two dipolar-coupled protons and the reader is referred to any text on nuclear magnetic resonance in the solid phase for a detailed treatment of the physics involved (see ref. 13). Interpreting the nuclear magnetic resonance results in terms of electrons, the dipole coupling yields a pair of lines located at magnetic fields given by

$$H = H_0 \pm 3g\beta(1-3\cos^2\theta)/4r^3 \qquad [1]$$

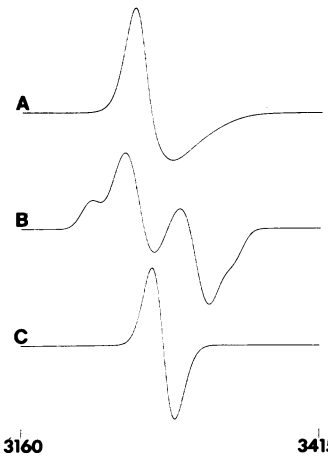

FIG. 4. Computer-synthesized spectra. (A) The best fit to noninteracting Hipip assuming $g_x = 1.9897$, $g_y = 2.0108$, $g_z = 2.0190$, $L_x = 25$ G (0.0025 tesla), $L_y = 15$ G (0.0015 tesla), $L_z = 7$ G (7×10^{-4} tesla). (B) The spectrum for two dipolar coupled SQ molecules assuming $g_\parallel = 2.0066$, $g_\perp = 2.0041$, $L_\parallel = 8$ G (8×10^{-4} tesla), $L_\perp = 11.5$ G (11.5×10^{-5} tesla), and $r = 7.71$ Å along $g_\parallel$. (C) The spectrum for isolated SQ assuming $g_\parallel = 2.0066$, $g_\perp = 2.0041$, $L_\parallel = 8$ G (8×10^{-4} tesla), and $L_\perp = 11.5$ G (11.5×10^{-4} tesla).

where $H_0 = h\nu/g\beta$, r is the distance between species, and θ is the angle between r and the applied magnetic field. Because the sample is a frozen solution, we assume that all orientations are equally likely and the resulting spectrum will be obtained by weighting the spectrum for any given orientation (θ,Φ) by the solid angle at that orientation. That is, the number of species located between θ and $\theta + d\theta$ and between Φ and $\Phi + d\Phi$ is given by $dN = N \sin\theta\, d\,\theta\, d\,\Phi/4\pi$. Using Eq. 1 to obtain $\sin\theta d\theta$ in terms of H and dH, one can obtain the number of species having absorptions centered between H and $H + dH$. If this distribution of line centers is convolved with a derivative line shape for each individual line, one obtains the classic dipolar line shape (see Fig. 4-10 of ref. 13). This is almost but not quite that shown in Fig. 4B. The latter spectrum shows slight anisotropies which we can understand when we realize that the outer peaks come from those molecules where $\theta \simeq 0$. If these molecules had slightly larger g-values, that would shift these peaks downfield and the resulting spectrum would be that of Fig. 4B. In other words, the nature of the experimental spectrum is such that the g-values parallel to r must be slightly larger than those perpendicular to r.

The dipole-dipole interaction between point electrons is given by

$$\mu_1 \cdot \mu_2/r^3_{12} - 3(\mu_1 \cdot r_{12})(\mu_2 \cdot r_{12})/r^5_{12}$$

where r_{12} is the separation between the two point electron and μ_1 and μ_2 are their magnetic moments, respectively. In the case at hand, if such an interaction is to be responsible for the structure in the EPR spectrum, the distance between the interacting spin systems must be of the same order as the dimensions of the unpaired electron distributions themselves; i.e., the magnitude of the interaction required is such that r_{12} must be less than 8 Å. Thus, it is necessary to take the expectation value of the above interaction over the unpaired-electron distributions, which at the moment are unknown. For the sake of simplicity, we will assume that the distribution has an axis of symmetry; hindsight will show that this assumption introduces errors in a synthesized spectrum less than an individual linewidth.

The Hamiltonian operator representing the above interaction is a second-rank tensor which can be decoupled and written as a product of a space part and a spin part. Invoking the spherical harmonic addition theorem, one can then integrate over the space part, and under the assumptions of axial symmetry and negligible g-value anisotropy this yields an effective spin Hamiltonian:

$$\mathcal{H} = D(1 - 3\cos^2\theta)\, S_{1_z} S_{2_z} - D(1\text{-}3\cos^2\theta)\,(S_1^+ S_2^- + S_1^- S_2^+)/4 \quad [2]$$

where θ is the angle between the axis of symmetry of the unpaired-electron distribution and the applied magnetic field and D is the expectation value of the axial term of the dipole–dipole interactions over the unpaired electron distribution, $D = (g_1 g_2 \beta^2/2)\langle(3z^2_{12} - r^2_{12})/r^5_{12}\rangle$ with z_{12} being the component of r_{12} along the symmetry axis of the unpaired-electron distribution.

With the insight provided by the above, a computer program was written in which the g-tensors for each species were permitted to be anisotropic and different from each other and r was permitted to take on any fixed orientation with respect to these g-tensors. (It should be noted that when the spin systems become nonidentical, the eigenfunctions are no longer pure singlet and triplet and the locations of the resonance lines and their intensities are no longer given by the expressions in the previous discussion.) The computer program treated the dipolar interaction by first-order degenerate perturbation theory, calculated the energies and transition probabilities, summed the resulting spectra from a representative set of orientations, and then convolved the resulting stick-spectrum with a derivative Gaussian line-shape to obtain the synthesized spectra as in Fig. 4B. To this spectrum for two interacting species must be added the spectrum for noninteracting Hipip (Fig. 4A) and possibly for noninteracting SQ (Fig. 4C) in unknown amounts before a comparison with the experimental spectrum is possible.

Numerous spectra were calculated, and the "best fit" to the spectrum in Fig. 3 from Complex II plus SQ is shown in Fig. 5A. This spectrum assumes the following model: The experimental spectrum is composed of three different components: (*i*) noninteracting Hipip (Fig. 4A); (*ii*) dipole coupled pairs of SQ (Fig. 4B) assumed to have axial g-tensors ($g_\parallel = 2.0066$, $g_\perp = 2.0041$) with r along $g_\parallel$ of both centers; and $\langle(3z^2_{12} - r^2_{12})/r^5_{12}\rangle = (1/7.71\text{ Å})^3$; and (*iii*) noninteracting SQ (Fig. 4C). These three components are then summed in the ratio of the numbers of species of 1.4:1.0:0.125 for Hipip, interacting SQ, and noninteracting SQ, respectively.

Although this model fits the data rather well, a slightly different model cannot be ruled out. This model, whose calculated spectrum is shown in Fig. 5B, also consists of a weighted sum. Here 1.4 units of Hipip are added to 1.0 unit of dipole interacting Hipip-SQ centers under the assumptions that the Hipip g-tensor is given by $g_x = 1.9897$, $g_y = 2.0108$, $g_z = 2.0190$ with linewidths at half maximum given by $L_x = 25$ G (25×10^{-4} tesla), $L_y = 15$ G (15×10^{-4} tesla), $L_z = 7$ G (7×10^{-4} tesla); the SQ g-tensor and linewidths are given by $g_\parallel = 2.0066$, $g_\perp = 2.0041$, $L_\parallel = 8$ G (8×10^{-4} tesla), $L_\perp = 11.5$ G (11.5×10^{-4} tesla); and the interaction parameter $\langle(3z^2_{12} - r^2_{12})/r^5_{12}\rangle = (1/7.71\text{ Å})^3$ with the axis of symmetry oriented 30° away from y toward the z axis. The spectrum shown has some similarities to the experimental data. However, the overall quality of the fit to the data is not as good as the first model. In particular, the lowfield part

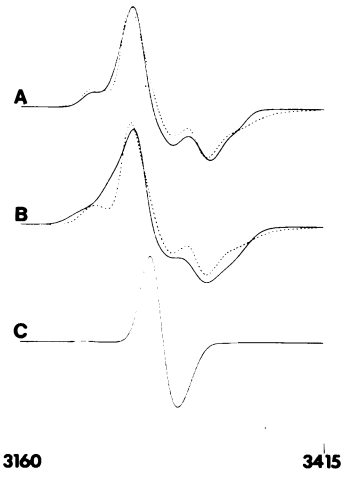

FIG. 5. Computer synthesized spectra (*solid lines*) and experimentally observed spectra (*dashed lines*) for Complex II plus SQ (Fig. 3). (A) The composite spectrum obtained by summing the spectra of Fig. 4A, B, and C in the ratio 1.4:1.0:0.125 by species, that is, this spectrum assumes two coupled SQs. (B) The composite spectrum obtained by adding the spectrum of noninteracting Hipip (Fig. 4A) to the spectrum obtained from a dipolar coupled Hipip and SQ pair using the parameters described in the *text* and a weighting ratio of 1.4:1. (C) The synthesized spectrum of a Hipip-SQ pair coupled by an isotropic exchange interaction (notice the extremely weak satellite lines) using the parameters described in the *text*.

of the spectrum is poorly reproduced. The small peak is too far to the left and both lowfield peaks appear to be too broad.

Finally, an isotropic exchange interaction (see ref. 14) model was calculated assuming an interaction $-2JS_1 \cdot S_2$ ($2J$ = 140 MHz) between Hipip and SQ and the above g-values and linewidths. The computed spectrum is shown in Fig. 5C. As one would expect from g-tensors so nearly equivalent, the exchange interaction has very little effect on the calculated shape of the EPR spectrum (the reader is reminded that an exchange interaction between identical spins has no effect on the transition energies) and does not show the splittings seen in the experimental spectra.

The accuracy of all the spectra calculated depends on the validity of the assumptions and approximations made. The first basic approximation made is that the moments are aligned along the spin directions in computing the dipole–dipole interaction. This introduces errors on the order of $(\mu/r^3)(\Delta g/g)$, which for this calculation are less than 1 G (10^{-4} tesla). The second assumption was that the spin distribution has an axis of symmetry that reduced the dipole–dipole interaction to those terms shown in Eq. 2. If this is not the case, there are additional terms that enter as second-order corrections to the energies. These latter corrections are of the order of $(g^2\beta^2/r^3)^2/g\beta H$, which is 1.5 G ($1.5 \times 10^{-4}$ tesla). Thus, we see that the approximations made in the spectral simulations introduce errors much less than the linewidths.

Identity of interacting species

The following evidence implicates SQ as one of the reaction partners: (*i*) We have never detected the typical EPR signal in ETP from which Q had been extracted, but after reincorporation of Q the signal can again be elicited. (*ii*) We have never observed the signal in Complex II, which does not contain significant amounts of Q, except on reoxidation of reduced Complex II with added Q. The evidence for the identity of the second reaction partner is ambiguous at this time. Although the consistently observed association of the typical EPR signal with the membrane-bound Hipip species suggests that Hipip is involved in the interaction, this does not prove that Hipip is necessarily the immediate reaction partner. Since the g-values of the Hipip and SQ signals are very similar and since we do not know in which way these values may be changed on interaction, we can only draw conclusions on the basis of the spectra of the noninteracting species, and doing so, our present computer simulations come out in favor of SQ-semiquinone interaction over SQ-Hipip interaction (compare Fig. 5A and B). Again, however, the identity of the second semiquinone species is not clear. The EPR signals of flavin semiquinone and SQ are sufficiently similar that either possibility is open. In our opinion the ambiguity concerning the second interacting partner can only be resolved when the characteristic signal is found in submitochondrial fractions in which flavin or Hipip or both are clearly absent. Since verification of any of the three possibilities that we propose here would introduce new aspects into considerations of mechanisms of mitochondrial electron transfer, we would like to communicate our findings at this stage. It seems particularly significant to us that the typical signals of interacting SQ are observed in whole heart tissue. EPR spectroscopy thus provides a means to verify the existence, and possibly also to study the function, of SQ in mitochondria or whole tissue where optical methods cannot be applied at this time.

1. Orme-Johnson, N. R., Orme-Johnson, W. H., Hansen, R. E. & Beinert, H. (1971) *Biochem. Biophys. Res. Commun.* **44**, 446–452.
2. Orme-Johnson, N. R., Hansen, R. E. & Beinert, H. (1974) *J. Biol. Chem.* **249**, 1928–1939.
3. DerVartanian, D. V., Morgan, T. V. & Brantner, R. V. (1974) *Biochim. Biophys. Acta* **347**, 497–502.
4. Slater, E. C. (1973) in *Oxidases and Related Redox Systems*, eds. King, T. E., Mason, H. S. & Morrison, M. (University Park Press, Baltimore, Md.), Vol. 2, pp. 794–796.
5. Sweeney, W. V., Bearden, A. J. & Rabinowitz, J. C. (1974) *Biochem. Biophys. Res. Commun.* **59**, 188–194.
6. Ruzicka, F. J. & Beinert, H. (1974) *Biochem. Biophys. Res. Commun.* **58**, 556–563.
7. Bäckström, D., Norling, B., Ehrenberg, A. & Ernster, L. (1970) *Biochim. Biophys. Acta* **197**, 108–111.
8. Crane, F. L., Glenn, J. L. & Green, D. E. (1956) *Biochim. Biophys. Acta* **22**, 475–487.
9. Norling, B., Glazek, E., Nelson, B. D. & Ernster, L. (1974) *Eur. J. Biochem.* **47**, 475–482.
10. Kröger, A. & Klingenberg, M. (1966) *Biochem. Z.* **344**, 317–336.
11. Mathews, R., Charlton, S., Sands, R. H. & Palmer, G. (1974) *J. Biol. Chem.* **249**, 4326–4328.
12. Gutowsky, H. S. & Pake, G. E., (1950) *J. Chem. Phys.* **18**, 162–170.
13. Hecht, H. G., (1967) in *Magnetic Resonance Spectroscopy* (Wiley, New York), pp. 84–89.
14. Wertz, J. & Bolton, J. R. (1972) in *Electron Spin Resonance* (McGraw-Hill, New York), pp. 250–252.